Quaternary Science Reviews 278 (2022) 107374

Contents lists available at ScienceDirect

Quaternary Science Reviews

journal homepage: www.elsevier.com/locate/quascirev

Climate adaptation of pre-Viking societies

Manon Bajard [a, b, *], Eirik Ballo [a, b], Helge I. Høeg [c], Jostein Bakke [d], Eivind Støren [d], Kjetil Loftsgarden [c], Frode Iversen [c], William Hagopian [b], Anne H. Jahren [b], Henrik H. Svensen [a, b], Kirstin Krüger [a, b]

[a] Department of Geosciences, University of Oslo, Oslo, Norway
[b] Centre for Earth Evolution and Dynamics, University of Oslo, PO Box 1028, Blindern, 0315, Oslo, Norway
[c] Department of Archaeology, Museum of Cultural History, University of Oslo, Oslo, Norway
[d] Department of Earth Science and Bjerknes Centre for Climate Research, University of Bergen, Allègaten 41, 5007, Bergen, Norway

ARTICLE INFO

Article history:
Received 19 July 2021
Received in revised form
3 January 2022
Accepted 4 January 2022
Available online 17 January 2022

Handling Editor: Yan Zhao

Keywords:
Palaeoclimate
Adaptation
Agriculture
Temperature
Dark ages cold period

ABSTRACT

Understanding how the Viking societies were impacted by past climate variability and how they adapted to it has hardly been investigated. Here, we have carried out a new multi-proxy investigation of lake sediments, including geochemical and palynological analyses, to reconstruct past changes in temperature and agricultural practices of pre-Viking and Viking societies in Southeastern Norway during the period between 200 and 1300 CE. The periods 200–300 and 800–1300 CE were warmer than the 300–800 CE period, which is known as the "Dark Ages Cold Period". This cold period was punctuated by century-scale more temperate intervals, which were dominated by the cultivation of cereals and hemp (before 280 CE, 420–480 CE, 580–700 CE, and after 800 CE). In between, cold intervals were dominated by livestock farming. Our results demonstrate that the pre-Viking societies changed their agricultural strategy in response to climate variability during the Late Antiquity.

1. Introduction

Understanding how earlier agricultural societies were impacted and adapted to past climate changes is critical to facilitate current and future climate transitions and sustain food production (Orlove, 2005; Costanza et al., 2007). While many studies link historical events, abandonment of settlements and collapse of societies to abrupt or long lasting climate variations (Haug et al., 2003; Buntgen et al., 2011; Toohey et al., 2016), less is known about long term trends in adaptation and resilience of past societies, and more specifically pre-Viking and Viking societies, when facing climate change.

The extensive research in the last decades on past climate and climate dynamics has led to greatly improved understanding of the drivers of natural climate variability. As a result of more accurate chronologies deciphered from tree rings and ice core records (Sigl et al., 2014, 2015; Büntgen et al., 2016), mineralogical and biological signals preserved in sedimentary sequences can be correlated more confidently with climate variables. However, the potential impact of the climate variability on societies is more challenging to prove, due to lack of regional evidence from both natural archives and archaeological sources, as well as firmly based interpretations relevant for understanding societal resilience. Archaeological evidence and historical documentation are valuable sources of information to study societal dynamics. They may pinpoint a series of single events and records but they often lack spatio-temporal resolution, continuity and duration when compared to climate reconstructions. Continuous regional records of environmental changes, serving as a framework for historical reconstruction are necessary to establish the link between single events, artefacts, chronicles and climate (Widgren, 2012).

Lake sediments represent highly valuable archives as they hold the potential to simultaneously record changes in climate, environment and human activities. Extracting and interpreting such information from the same archives allows past climate/society interactions to be studied at the same scales in space and time, enabling us to assess potential causal links. By doing all the analyses

* Corresponding author. MetOs Meteorology and Oceanography section, Department of Geosciences, Faculty of Mathematics and Natural Sciences, University of Oslo, Kristin Bonnevies hus, Blindernveien 31, 0371, Oslo, Norway.
E-mail address: manon@geo.uio.no (M. Bajard).

https://doi.org/10.1016/j.quascirev.2022.107374

on the same sedimentary archive and chronology, we overcome the uncertainty associated with different age/depth models that is problematic when comparing records of past climate and human activities.

We focus our study on the first millennium of the Common Era including the onset of the Viking society because this time period encompasses several climatic anomalies, especially between 250 and 600 CE (Buntgen et al., 2011; Helama et al., 2017a). In the Northern Hemisphere, numerous studies point towards a cold climate anomaly centred in the mid-first millennium (Helama et al., 2017a; Riechelmann and Gouw-Bouman, 2018). This period, termed the "Dark Ages Cold Period" (300–800 CE) by the natural sciences and "Late Antiquity" by the historians, took place between the Roman (1–375 CE) and Medieval (c. 800–1300 CE) periods. Both the Roman and Medieval periods are well known for their expanded society and their respective warm climate (i.e. Roman Warm Period and Medieval Warm Period) (Buntgen et al., 2011; Luterbacher et al., 2016). However, less is known about the societies that evolved in Scandinavia between these more temperate periods. The term "Dark Ages" reflects fewer available written sources and historical accounts, so "historians were not able to shed light on it" (Mommsen, 1942). The Dark Ages Cold Period covers the periods coined the Migration period (400–568 CE) and the Merovingian/Vendel period (568–800 CE) in Scandinavian history.

Between 300 and 800 CE, a globally cold period referred as the Late Antique Little Ice Age (LALIA) has recently received more attention (Büntgen et al., 2016; Helama et al., 2017b; Newfield, 2018; Peregrine, 2020). The LALIA started around 536 CE, driven by a series of unidentified large volcanic eruptions in 536, 540, 547 and 574, continuing until around 660 CE (Büntgen et al., 2016). Reported impacts suffered by society include crop failure, famine and farm abandonment. In Estonia, the cultivation of rye was increased in the second part of the first millennium in response of the sudden cooling in the mid-6th century, and the population was reduced, not recovering until the 9th century (Tvauri, 2014). Several palynological studies from Estonia, Sweden, Norway, Lithuania, Denmark and Poland show decreasing human activity and forest regeneration in the agricultural landscape around the 6th century but they often lack accurate dating, and have poor sampling resolution for this period (Königsson, 1968; Niinemets et al., 2002; Stancikaite et al., 2004; Kupryjanowicz, 2007; Tvauri, 2014; Galka et al., 2014; Wieckowska-Lüth et al., 2017). Changes in the organisation of society are also evidenced in the archaeology of the Norse. Archaeologists have reported a division of farms into smaller production units in central areas and complete abandonment in marginal areas (Solberg, 1998; Iversen, 2016). A decrease in human activities is also reported from a lake sediment study from Lofoten (Northern Norway) from 550 CE to around 825 CE (D'Anjou et al., 2012). In Northern Norway and Finland, the population, which relied more on fishing, animal husbandry and hunting, appears to have been less impacted by this cooling (Tvauri, 2014; Wickler and Narmo, 2014). They were not dependent on crop production, which was already difficult in the climates of Northern Scandinavia. In Southeastern Norway, pollen analysis has been used to investigate Holocene vegetation change, but there are no local reconstructions of climate available (Wieckowska-Lüth et al., 2017). Therefore, more proxy records of both climate and environmental changes are needed to shed light on the societies of the Dark Ages and the onset and decline of the Viking Age (Helama et al., 2017a).

In this paper, we present new data on how the ancestors of the Viking societies adapted to the climate variability of the Late Antiquity. We base our conclusions on a unique multi-proxy study of carbon 14-dated sediments from Lake Ljøgottjern in Southeastern Norway. By combining analyses of geochemical composition and palynology, we derive proxies for temperature and changes in agricultural practices. Based on the results, we discuss how climate variability impacted the socio-environmental interactions.

Lake Ljøgottjern (11°8′18″E, 60°8′54″N) is located in Southeastern Norway (Fig. 1a) at 185 m a.s.l., 2.5 km SSE from Oslo Airport and 1.5 km W of Jessheim. The lake (0.018 km^2) occupies a kettle-hole formed on the distal part of the Gardermoen delta by the melting of a buried dead-ice block left by the retreat of the Scandinavian Ice Sheet c. 9500 years ago (Longva and Thoresen, 1989). The lake has a maximum depth of 18 m with a very small (0.15 km^2) endoreic catchment (Fig. 1b). The mean annual temperature in Jessheim is 4.5 °C and annual mean precipitation is 807 mm (https://en.climate-data.org/europe/norway/akershus/jessheim-25749/#climate-graph). Snow normally covers the area from December to April and the lake is approximately ice-covered during the same period. The lake is surrounded by agricultural crops and farms (Fig. 1c). The oldest settlements in the close surroundings are dated to the Bronze Age (c. 1800–500 BCE, Helliksen, 1997; Directorate for Cultural Heritage, 2020, ID96260). Four farmsteads (Haug, Ljøgot, Eastern Hovin and Northern Hovin) are known from historical and archaeological records and dated to the first millennium (Fig. 1c). The largest burial mound of Northern Europe, Raknehaugen, was built in the mid-6th century on the shore of the lake (Skre, 1997). The mound is 15 m high, 77 m in diameter, and consists of three substantial layers of timber (chiefly pine, the rest being mainly birch), with soil and sand from the surroundings (Nydal, 1959; Skre, 1997). The excavator Sigurd Griegs's consulting engineer Harald Alfsen, estimated that the upper and largest timber-layer alone consisted of c. 25,000 logs (Grieg, 1940; Ording, 1941; Johnsen, 1943).

2. Materials and methods

2.1. Coring

Two coring campaigns were undertaken to retrieve sediments from the deepest part of Lake Ljøgottjern (c. 18 m, same location for both cores) in November 2018 and May 2019, respectively, when the lake was ice-free. The lake corings were done from a coring platform using a modified piston corer equipped with a 110 mm diameter, 6 m long PVC tube (Nesje, 1992). In addition, a 90 mm-UWITEC gravity corer was deployed to capture the sediment/water interface during both campaigns. The long piston cores were cut into four sections and sealed in the field for transport to the EARTHLAB at the University of Bergen, where they were split lengthwise, visually described and logged. The gravity cores were correlated with the upper part of the long piston cores and a composite stratigraphy of c. 6 m was constructed for each coring and named LJØ118 and LJØ119. One half of each core section was used for non-destructive analyses (XRF core scanner) and the other half for sampling and destructive analyses (carbon 14, loss-on-ignition, stable isotopes and pollen analysis).

2.2. XRF geochemistry

Both cores were scanned at EARTHLAB at the University of Bergen with an ITRAX core scanner from COX Analytics, at 200 μm sampling resolution for LJØ118 and 1000 μm for LJØ119. The surface of the cores was cleaned and smoothed before they were covered with an ultra-thin transparent film to avoid contamination and desiccation of the sediment. The geochemical data were obtained with different voltage and current settings for optimising the sensitivity of the analysis to the sediment for the most interesting geochemical elements. These settings were adjusted to 35 kV and 30 mA for 10 s with a Mo tube to detect Ca, Ti, K, Si, Fe, Mn. Data of LJØ118 were averaged every 5 measures to get the same resolution

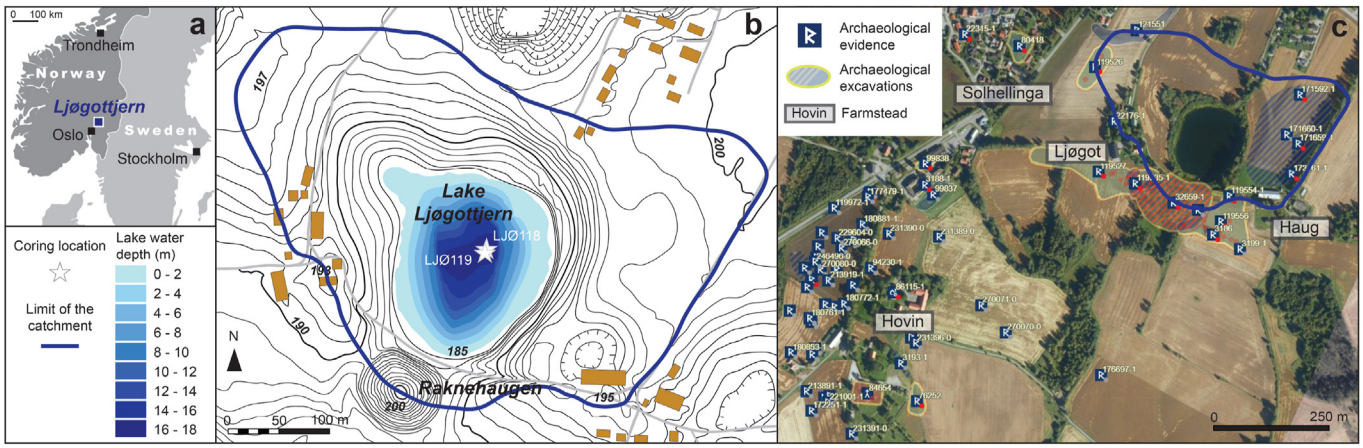

Fig. 1. Location of the study area. a Location of Lake Ljøgottjern in Southeastern Norway, **b** topographic map of the area, bathymetry of the lake and location of the sediment cores in the lake, marked with stars. **c** aerial view of the catchment and location of the archaeological sites of the surroundings from the Norwegian cultural heritage database "Askeladden".https://askeladden.ra.no/

as LJØ119 (i.e. 1 mm). The correlation of depths between the two sequences was performed using QAnalyseries 1.4.2 (Kotov and Paelike, 2018), using variations in Ti, Fe and Mn and visual observations of the sediment. Log-ratios of element intensities were calculated for Ca/Ti and Si/Ti to provide the most robust signals of relative changes in chemical composition (Weltje and Tjallingii, 2008). The normalisation to Ti was chosen here to remove the signal from terrestrial inputs of the catchment to allow the lake productivity to be traced (Bonk et al., 2021).

2.3. Loss-on-ignition

Loss-on-ignition (LOI) analysis was done for every 0.5 cm (i.e. c. every 5 years) between 0.83 and 2.17 m and then for every 1.0 cm down to a depth of 2.5 m in LJØ118. Sediment samples were dried overnight at 105 °C before ignition at 550 °C for 1 h. The organic matter (OM) content was calculated based on the difference before and after ignition, while the carbonate content was calculated after one more hour of ignition at 950 °C, following Dean Jr. (1974). Dry bulk density was calculated on the same samples by weighing a known volume of sediment after drying at 105 °C.

2.4. Organic geochemistry

Stable isotopes of carbon and nitrogen were measured on 30 dried and crushed samples from core LJØ118 within the CLIPT Lab at the University of Oslo using a Thermo Fisher Scientific DeltaV Isotope Ratio Mass Spectrometer configured with a Flash Elemental Analyzer. Samples for $\delta^{13}C$ analysis were acidified with a 10% HCl solution to remove carbonates prior to analysis. Amounts of 0.4 and 2 mg of sediment were sealed into tin capsules for $\delta^{13}C$ and $\delta^{15}N$ analysis, respectively. All samples were measured in duplicate. Stable isotope values were reported in standard δ-notation [$\delta = R_{sample}/R_{standard}$-1 x 1000], in units of per mil (‰), with R_{sample} and $R_{standard}$ representing the isotope ratio (13C/12C or 15 N/14 N) in the sample or international standard (VPDB for carbon and AIR for nitrogen), respectively. The total C and N were also measured and the C/N ratio was calculated.

2.5. Pollen analysis

A total of 65 samples of 1 cm^3 were collected at 2 cm (c. 20 years) intervals from the LJØ119 sequence for analysis of pollen and Non-Pollen Palynomorphs (NPPs). The samples were prepared as described in Faegri and Iversen (1989). Tablets of exotic spores (*Lycopodium clavatum*) were added to each samples to calculate concentrations in *Sordaria* ascospores and charcoals (Stockmarr, 1971). At least 500 pollen grains of terrestrial plants were identified and counted in each sample manually. The nomenclature of pollen-types are mostly from Lid and Lid (1994). The identification keys that were used are Faegri and Iversen (1966) and Beug (1961) for the cereals.

Pollen counts were expressed as percentages of the total sum of pollen grains of each sample. Lowland taxa are included in the total sum of pollen. First, the identified taxa were separated into different groups (i.e. trees, shrubs, Poaceae, pasture/grassland, cultivated, other) to build a synthetic diagram. Then, by applying a principal component analysis (PCA) on a selection of the pollen taxa, NPPs analyses and variables from the geochemistry, the statistical relationship between vegetation, human activity and climate during the studied period was outlined. The analyses were carried out using the software "R" version 2.13.1 (R Development Core Team, 2011) and the script package RcmdrPlugin.FactoMineR.

2.6. Chronology

The chronology of the sediment sequence is based on four ^{14}C measurements on terrestrial plant macroremains from core LJØ118. AMS (accelerator mass spectrometer) radiocarbon dates were performed by the Tandem Laboratory at Uppsala University. The ^{14}C ages were calibrated using the IntCal20 calibration curve (Reimer et al., 2020). The age-depth model for the LJØ118 sequence was generated using R software and the R code package 'Bacon' 2.4.3 (Blaauw and Christen, 2011). In the age model, the top of the core was set to the year of coring, i.e. 2018 CE. The chronology of core LJØ119 was deduced from the age model built on core LJØ118. The depths of both sequences were correlated using the variations of the XRF geochemistry (i.e. Ti, Ca, Fe and Mn intensities).

3. Results

3.1. Coring and chronology

Two cores of approximately 6 m length (denoted LJØ118 and LJØ119) were retrieved from the same location in the lake in 2018 and 2019 (Fig. 1). The upper 3 m of sediments were analysed for this

study. Detail of the samples and calibrated ages are presented in Table 1. The age/depth model of the sediment sequences is constrained by four ^{14}C-dated plant macrofossil samples from core LJØ118 (Fig. 2). The resulting age-model is linear with a mean sedimentation rate of 1.25 mm.yr^{-1} (Fig. 2). The top 2.5 m of sediment covers the last 2000 years. The section of sediment between 90 and 227 cm spans the period 200–1300 CE.

3.2. Sedimentology

The complete description of the lithology and geochemistry of the studied section is presented in Supplementary Fig. 1. In short, the sediments between 90 and 227 cm consist of dark silt materials continuously punctuated by millimetre-to centimetre thick-orange horizons and grey laminations. The organic matter (OM) content measured by loss-on-ignition (LOI) varies between 30% and 70%, with the highest values at the bottom and top of the section (Fig. 4 and Supplementary Fig. 1). The bulk sediment composition was measured on both cores using an ITRAX XRF core scanner. Ca intensities are high in the bottom (227-212 cm, 300–200 CE) and in the top part of section (175-105 cm, 1200–600 CE). Ti and K intensities co-vary with lower intensities in the top of the section (above 145 cm, 850 CE) than in the lower part. Prominent peaks in Ca, Ti and K are measured at 210 cm (c. 330 CE). The C/N ratio is higher in the bottom of section (200–550 CE), with a maximum of c. 18, and gradually decreasing to approximately 12 in the uppermost section of the core (Fig. 4 and Supplementary Fig. 1).

The variations in the Ti measured using the XRF core scanner show several high peaks on the first 50 cm of the sediment core (Fig. 1). These peak are related to historical floods documented in the region (Nesje et al., 2001; Bøe et al., 2006; Engeland et al., 2020). The dates of the floods and the age given by our age model are comparable (<10 years). In particular, the Ti peak related to the largest flood known in Norway, “Stor-ofsen”, is dated from 1790 with our carbon 14 age-model for the year 1789 CE. These peaks supports the validity of our age-depth model and allow us to identify other downward peaks of Ti as past flood events (e.g. at c. 330 CE). These floods are related to heavy rainfall during the snow melt period (Engeland et al., 2018). As Lake Ljøgottjern does not have any inlet or outlet, the large input of water is increasing the water level of the lake, flooding the shores of the lake, bringing large amount of terrestrial sediments that are traced by Ti in the lake sediments (Engeland et al., 2020).

3.3. Palynology

A synthetic palynological diagram was constructed (Fig. 3) with the percentages of pollen of trees, shrubs, Poaceae, a group of pasture/grassland indicators (including *Rumex acetosa*, *Rumex longifolius*, *Plantago major*, *Plantago lanceolata*, *Artemisia*, *Chenopodiaceae* and *Urtica*), cultivated taxa (including *Cannabis*, *Hordeum/Avena*, *Triticum*, *Secale*, and *Linum*), and finally a group comprising all other pollen grains (see Supplementary Fig. 2 for the complete pollen diagram).

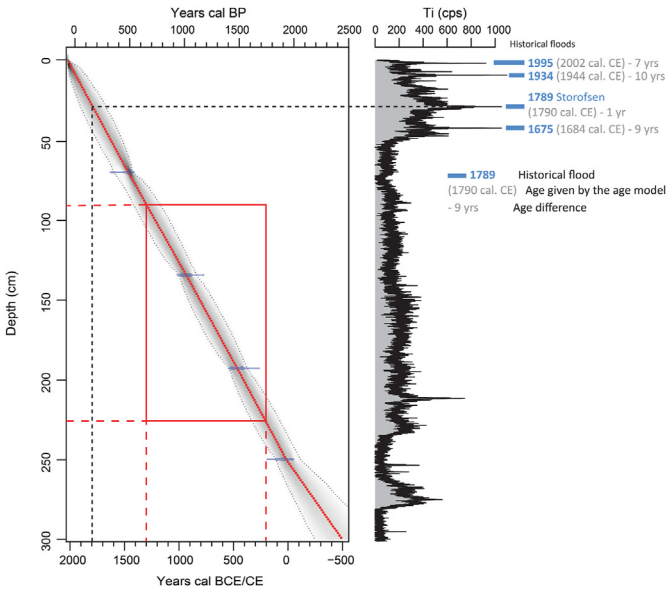

Fig. 2. Age/depth model of Lake Ljøgottjern sediment sequence. Represented with Bacon R package. The section in the red rectangle corresponds to the study period 200–1300 CE. XRF geochemistry of Ti in counts per second (cps). Historical floods from the literature (Nesje et al., 2001; Bøe et al., 2006; Engeland et al., 2020). (For interpretation of the references to colour in this figure legend, the reader is referred to the Web version of this article.)

There is a notable change in the pollen assemblage around 750–800 CE (Fig. 3). Before 750 CE, tree pollen represents 77% of the pollen sum, while after 750 CE the average decreases to 65% of the total. The tree pollen mainly represents *Pinus* and *Betula* (Fig. 3). *Alnus* presents an average of pollen around 10% between 200 and 300 CE, then decreases to a minimum around 570 CE (5%), and increases to a maximum (12%) at 650 CE. Percentages of pollen of *Alnus* decrease between 650 and 700 CE and remain low afterward with 4% of the pollen sum in average. The percentage of *Picea pollen* increases between 200 and 450 CE (from 1 to 7%), with the value remaining stable between 450 and 800 CE before increasing again after 800 CE (up to 14%).

The percentage of shrub pollen averages <2% before 650 CE and 3% between 800 and 1300 CE (Fig. 3), but increases from 2 to 12% between 650 and 800 CE. In the same period, Poaceae pollen also increases, from 9 to 18%.

The concentration of charcoal particles is higher (between 80,000 and 120,000 no.cm^{-3}) during the periods 200–400 CE (with a very high variability), 500–750 CE, and 1000–1300 CE and lower in the periods in between (20,000 to 40,000 no.cm^{-3}).

The pollen sum of ruderal species varies between 2 and 7%, with minima before 250 CE, between 400 and 450 CE, and around 600 and 700 CE (Fig. 3). Percentages are relatively stable (c. 3%) between 450 and 600 CE, then increase until 950 CE, after which they remain

Table 1
Radiocarbon ages for Lake Ljøgottjern sediment sequence.

Lab number	Sample name	Core depth (cm)	Sample type	δ^{13}C‰ V-PDB	^{14}C age BP	Min. age (cal. BP)	Max. age (cal. BP)	Min. age (cal. CE)	Max. age (cal. CE)	Mean age (cal. CE)
Ua-60967	LJP118-I/IV-21,5 −22 cm	70.25	Leaf/bark	−23,6	431 ± 30	452	526	1498	1424	1461
Ua-60968	LJP118-I/IV-86-86,5	134.75	Grass and some leaves	−27,9	1115 ± 32	956	1071	994	879	936.5
Ua-60969	LJP118-II/IV-12cm	193	Aquatic plant	−26,8	1623 ± 31	1406	1547	544	403	473.5
Ua-60970	LJP118-II/IV-69cm	250	Leaves/bark, seed	−24,8	1970 ± 31	1827	1949	123	1	62

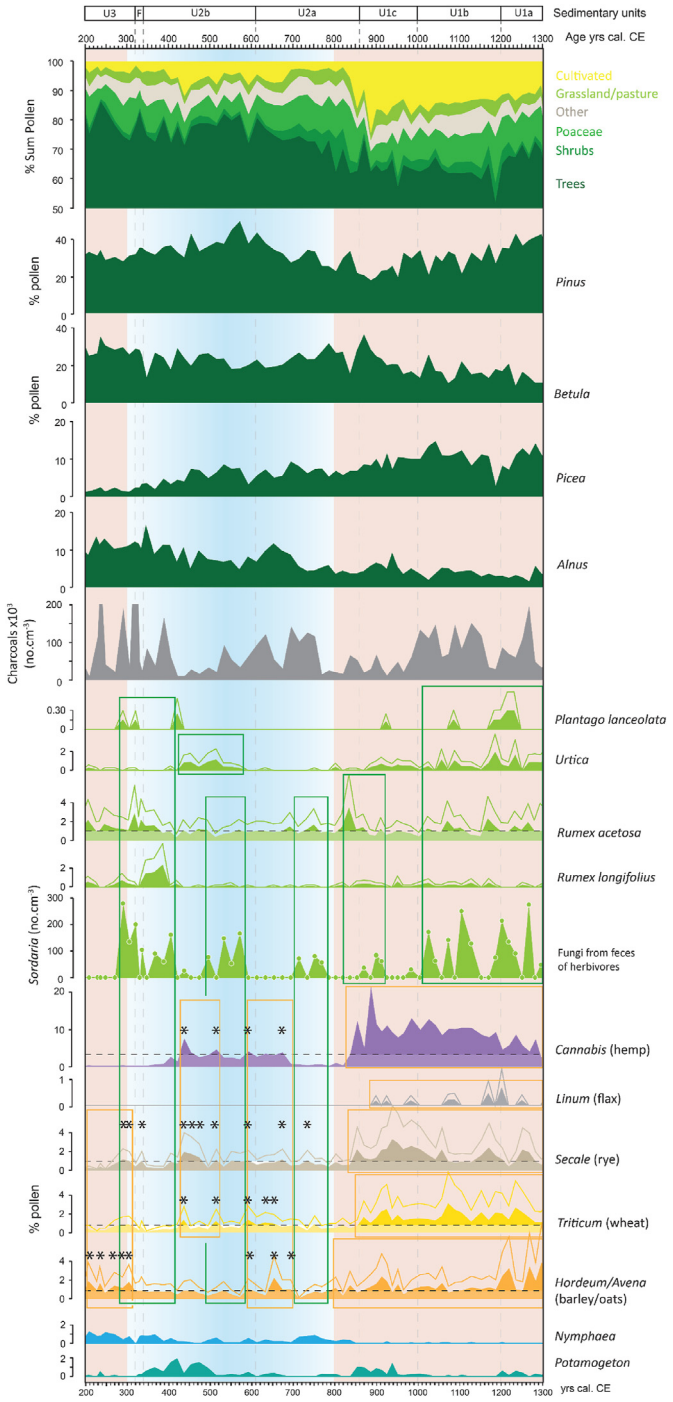

Fig. 3. Palynology of Lake Ljøgottjern. Synthetic pollen diagram and detail of a selection of taxa including the percentages of Pinus, Betula, Alnus, Picea, the concentration of charcoal particles, percentages of Plantago lanceolata, Urtica, Rumex acetosa, Rumex longifolius, the concentration of Sordaria, percentages of the cultivated Cannabis, Linum, Secale, Triticum, Hordeum/Avena, and the aquatic plants Nymphea and Potamogeton. The single curve above some taxa is an exaggerated curve x2. Horizontal dotted lines correspond to the median of the corresponding taxa for the period 200–1300 CE. Stars indicate percentages of pollen of hemp and cereals above median before 800 CE. We have framed periods with higher occurrence of pollen of cereals and hemp (orange) and Sordaria (green). Sedimentary units refer to the lithology in Supplementary Fig. 1. (For interpretation of the references to colour in this figure legend, the reader is referred to the Web version of this article.)

stable at c. 4% until 1300 CE. In detail, *Urtica* (needles) presents higher pollen percentages in the period 400–550 CE and after 800 CE. Percentages of *Rumex acetosa* are higher during the periods 250–400 CE, 650–750 CE, 800–900 CE and after 1000 CE. Pollen of *Rumex longifolius* are mainly higher between 250 and 400 CE. The spores of fungi *Sordaria* are mainly found during five periods: 280–420 CE, 480–580 CE, 700–780 CE, 860–920 CE and 1000–1300 CE, with the highest concentrations in the two first periods and the last one (Fig. 3).

Percentages of pollen of cultivated taxa are around 2% between 200 and 400 CE and between 650 and 800 CE (Fig. 3). Percentages are higher between 400 and 650 CE (up to 11%, 5% in average), and increase after 800 CE with an average of 14% and a maximum of 24% recorded at 885 CE. Pollen of cultivated taxa are dominated by *Cannabis* (hemp). In detail, *Hordeum/Avena* (barley or oats) is recorded above median between 200 and 300 CE. Pollen percentages of *Secale* (rye), *Triticum* (wheat) and *Cannabis* are recorded at least twice above median between 420 and 520 CE. Pollen percentages of *Triticum*, *Hordeum* and *Cannabis* are at least once above median between 580 and 680 CE. After 850 CE, percentages of pollen of *Cannabis*, *Secale*, *Triticum* and *Hordeum/Avena* are regularly above median. Pollen percentages of *Linum* (flax) are recorded sporadically after 885 CE. Among aquatic plants, percentages of pollen of *Nymphea* (c. 0.5–1%) are recorded between 200 and 850 CE and much less after this date (Fig. 3). Pollen percentages of *Potamogeton* (c. 1–2%) are mostly detected between 300 and 500 CE, 850 and 950 CE, and between 1200 and 1300 CE.

4. Discussion

4.1. Pollen and NPPs classification, indicators and limitations

The high-resolution analysis of pollen and NNPs allows to trace agricultural practices. In particular, we examined the pollen of *Hordeum/Avena, Secale, Triticum* and *Cannabis/Humulus* to trace cultivation of cereals and hemp (Fig. 3). We cannot dissociate the pollen of *Hordeum* and *Avena*, nor the pollen of *Cannabis* (hemp) and *Humulus* (hop). However, *Humulus* is wild growing, but not very common in Norway. When one or two grains are found in a few samples, those are associated to wild-growing *Humulus* in the pre-historical period (see ter Schure et al., 2021). For beer production, only female plants of hop are used, i.e. no pollen is produced. When there are many pollen of this type in a sample, it means that the plants are used for fiber-production. The whole plant is dipped out in the water, and lots of pollen flushes into the water. Both *Humulus* and *Cannabis* were used for fiber production. In Lake Ljøgottjern the DNA analysis of the same lake sediment sequence shows that *Humulus* was used in the beginning, around 300–400 cal CE, and then only *Cannabis* (ter Schure et al., 2021). Therefore, we assume that the pollen of *Cannabis/Humulus* found in the sediment of Ljøgottjern are mainly from cultivated *Cannabis* (Fig. 3). The DNA analysis of the sediment also suggest that *Hordeum* was more commonly cultivated than *Avena* (ter Schure et al., 2021).

To trace grazing activities, we analysed ascospores of *Sordaria* and pollen indicators of grassland/pasture as *Rumex*, *Plantago* and *Urtica* (Fig. 3; Doyen and Etienne, 2017).

Rumex species are divided into two groups, *Rumex acetosa* and *Rumex acetosella*, called *Rumex acetosa* and *Rumex longifolius* respectively. In the area of Lake Ljøgottjern, we do not have water living species of *Rumex*. *Plantago major* contains also *Plantago media*, but not other species. *Plantago lanceolata* includes only *Plantago lanceolata*. There are some other *Plantago*-species in Norway, but their pollen look differently. *Urtica* and *Rumex acetosella* are indirect grassland/pasture indicators. They are not widely eaten by

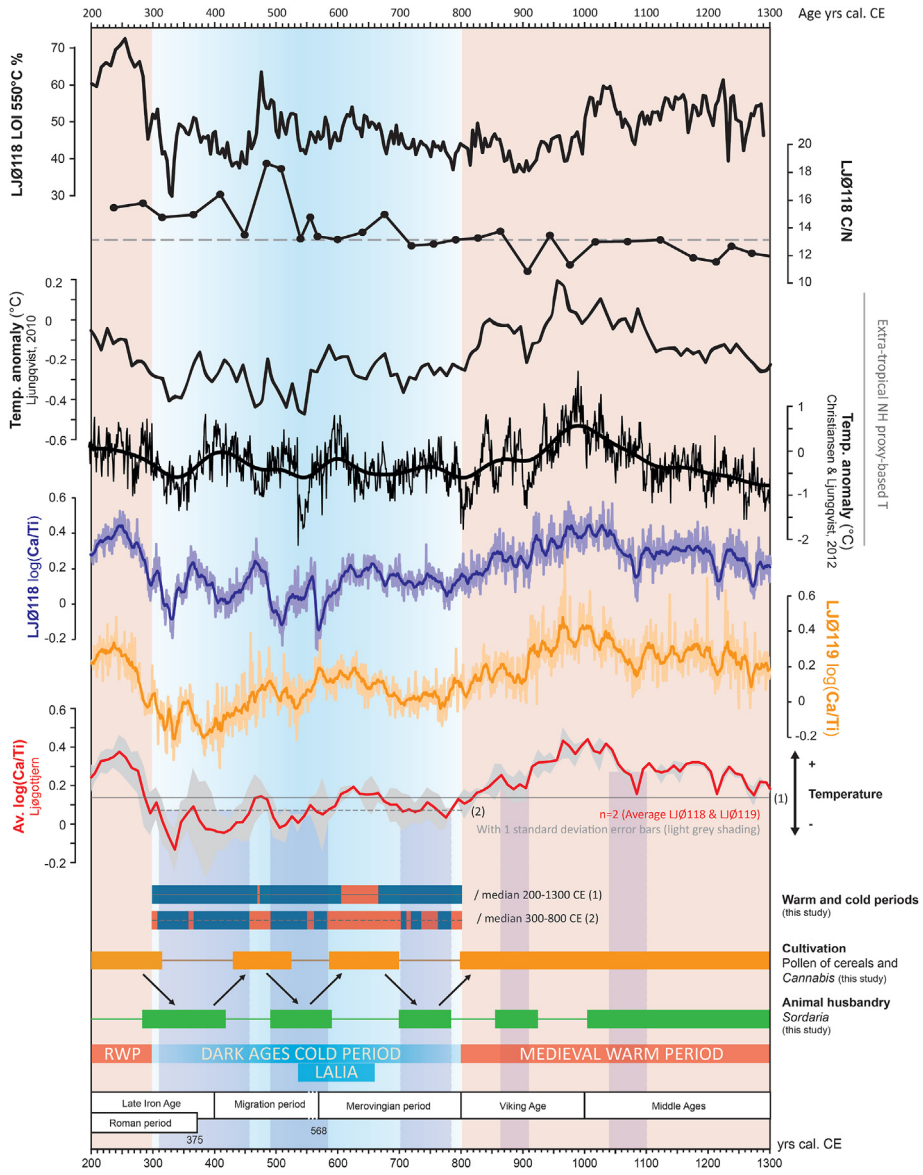

Fig. 4. Temperature reconstruction from Lake Ljøgottjern. Loss-On-Ignition (LOI) and C/N ratio measured in LJØ118 core. Temperature change recorded in Lake Ljøgottjern inferred from the record of log(Ca/Ti) in sediment sequences LJØ118 (yellow curve) and LJØ119 (blue curve), and from the average of log(Ca/Ti) from LJØ118 and LJØ119 (red curve) compared to the temperature anomaly reconstructed from proxy-based data for the extra-tropical North Hemisphere from Ljungqvist (2010) and Christiansen and Ljungqvist (2012). Periods dominated by animal husbandry or cultivation are adapted from Fig. 3. (For interpretation of the references to colour in this figure legend, the reader is referred to the Web version of this article.)

cattle but grow in areas enriched in nitrogen, which corresponds to areas where animals were standing for a long time and defecating.

Sordaria ascospores are, with *Sporormiella* and *Podospora*, mainly composed of coprophilous species and among the most common ascospores encountered on dung (Cugny et al., 2010). They are among the most robust indicators for grazing activities and their abundance could be related to the size of the cattle (Cugny et al., 2010; Etienne et al., 2013). Strict coprophilous fungi, as *Sporormiella* or *Podospora* have not been analysed in this study. *Sordaria* is not considered as a strict coprophilous fungi but has been shown to be mainly coprophilous (Cugny et al., 2010; Doyen and Etienne, 2017; Shumilovskikh and van Geel, 2020). *Sordaria* can also originate from decaying wood but very few samples contains *Sordaria* before the onset of agriculture around Lake Ljøgottjern c. −300 cal. BCE (Supplementary Fig. 3 and text, ter Schure et al., 2021). From c. −300 cal. BCE (2200 cal. BP), the variations in *Sordaria* concentration follow closely the development of human activities, as reflected by the change in pollen (decrease of the tree pollen, increase in anthropochores, apophytes, forbs and graminoids), increase in charcoal, erosion (Ti), and appearance of DNA of livestock (Supplementary Fig. 3, ter Schure et al., 2021). Pollen of *Plantago lanceolata* and *Plantago major*, plus the DNA of *Plantago* were also found only after −300 cal. BCE/CE (ter Schure et al., 2021; this study). This long-term multiproxy analysis of the sediments allows us to be confident on the association of *Sordaria* to husbandry during our study period from 200 to 1300 cal. CE. In the end, as Lake Ljøgottjern and its catchment are small, the record of pollen and NPPs must be local, reflecting the nearby development of activities (Sugita, 1994; ter Schure et al., 2021).

4.2. Sources of the sediments

The multiproxy geochemical analysis of the sediments of Lake Ljøgottjern allows fingerprinting of sediments sources. Ti and K, which show very similar variations in XRF count rates (Supplementary Fig. 1), are associated with the terrigenous part of the sediment. These elements can be used to trace erosion in the catchment, which is driven by the interplay of precipitation and human disturbance (Arnaud et al., 2016; Bajard et al., 2016). Ti and K are higher in the period 200–850 CE than in the period 850–1300 CE (Supplementary Fig. 1), indicating more erosion between 200 and 850 CE. Our pollen data show more human activity (higher percentage of cereal pollen) after 850 CE, but lower erosion (lower Ti and K), and conversely in the period 200–850 CE, suggesting that erosion is not associated with more human activity and thus, could be associated with precipitation. This hypothesis is supported by the higher precipitation recorded in Southern Norway around 200–850 CE (Støren and Paasche, 2014) and by the higher summer precipitation for the period 200–850 CE in Europe compared to the period 850–1300 CE on average (Büntgen et al., 2021). The large peak in Ti, K and Ca in section F around 330 CE could be associated with an extreme precipitation and/or snow melt event, accentuating runoff and erosion. This hypothesis is supported by the peaks in Ti count rates close to the top of the sediment core, which are linked to historical flood events (Fig. 2).

The organic matter in the sediments can have two origins, in wash of terrestrial material and the biological productivity in the lake, which can be differentiated by the C/N ratio. The terrestrial organic matter coming from the surrounding vegetation and soils typically has a C/N between 14 and 20, whereas autochthonous lacustrine organic matter has a C/N between 4 and 10 (Meyers and Teranes, 2002). The organic matter during the period 200–700 CE has a C/N closer to terrestrial vegetation than the organic matter recorded after 700 CE (Fig. 4). After 800 CE, the increase in organic matter content combined with a low C/N ratio indicates an increase in the productivity of the lake (Fig. 4). The synchronous increase in $\delta^{13}C$ further supports this hypothesis (Lücke et al., 2003). The peaks in organic matter, C/N and $\delta^{13}C$ between 470 and 520 CE indicate a major input of terrestrial organic matter to the lake, which could be linked to the construction of the Raknehaugen burial mound in the 6th century (Fig. 4 and Supplementary Fig. 1).

4.3. Record of temperature in the lake sedimentary archive in the period 200–1300 CE

The lake primary productivity is dependent on climate and nutrient availability (Adrian et al., 2009; O'Beirne et al., 2017), and we can use it to reconstruct the temperature changes. It is possible to quantify the primary productivity with the biogenic component of Ca and Si. Both Ca and Si can be used by micro-organisms in the lake and be recorded in the sediments. The biogenic production of Si is mainly associated to diatoms, which are commonly associated with carbonate deposits in lakes (Gierlowski-Kordesch, 2010). The biogenic production of Ca could be linked to algae, through heterogeneous nucleation (Stabel, 1986; Davaud and Girardclos, 2001). For example, Haptophytes are known for their calcareous exoskeleton and their production of alkenones used for temperature reconstruction (Theroux et al., 2010). However, Ca and Ti are also transported directly into the lake as solid particles eroded out of the catchment. When normalised to Ti, which is sourced only from the terrigenous part of the lake sediment, it is possible to quantify the biogenic component of Ca and Si in the sediment (Stabel, 1986). Ca/Ti and Si/Ti can therefore be used as proxies for the primary productivity in the lake.

Log transformed of Ca/Ti and Si/Ti show similar variations in both the LJØ118 and LJØ119 cores, with higher values between 200 and 300 CE, and after 800 CE, and lower values between 300 and 800 CE (Fig. 4 and Supplementary Fig. 4). The two log transformed ratios follow closely the temperature reconstruction by Ljungqvist (2010) and Christiansen and Ljungqvist (2012), which are based on various climate proxies (e.g. tree-ring, lake sediments) from the extra-tropical Northern Hemisphere area (Fig. 4).

A log-linear regression of the recorded ratios with the temperature data of Ljungqvist (2010) for the period 200–1300 CE shows significant positive correlations for both ratios, with correlation coefficients of $r^2 = 0.3$ (P value < 0.01) for Si/Ti and $r^2 = 0.5$ (P value < 0.01) for Ca/Ti (Supplementary Fig. 4). The weaker correlation of Si/Ti to the temperature record may be explained by more noise in the Si measurements, as Si is among the lightest elements of the periodic table of elements, and in the lower end of the sensitivity range of the ITRAX XRF core scanner when using a Mo tube. Si is also found as phytoliths in lake sediments, which originates from the terrestrial vegetation (e.g. Poaceae, cereals) and therefore does not only reflect the biogenic production of the lake. For these reasons, the ratio Ca/Ti is preferred for tracing changes in local surface air temperature. The organic matter of the sediment, as measured with the Inc/Coh ratio and LOI, shows very similar variations to the Log(Ca/Ti) and likewise increases significantly after 800 CE, while the C/N ratio is decreasing, confirming the increase in lake productivity (Fig. 4 and Supplementary Fig. 1).

The record of the Log(Ca/Ti) in both the LJØ118 and LJØ119 sequences was averaged to obtain a climate proxy with n = 2 samples from the same lake. The standard deviation of the temperature anomaly is shown in grey in Fig. 4, reflecting the differences in Ca/Ti between the two sediment sequences.

The resultant plots from the analyses described above show that the temperature at Ljøgottjern was higher between 200 and 300 CE and between 800 and 1300 CE and lower between 300 and 800 CE, in agreement with other records covering the Northern Hemisphere (Riechelmann and Gouw-Bouman, 2018). The colder period between 300 and 800 CE matches the previous definition of the Dark Ages Cold Period (Helama et al., 2017a). The highest mean temperature is recorded between 950 and 1000 CE, as also found by Ljungqvist (2010). During the cold period 300–800 CE, relatively warmer intervals are defined at Ljøgottjern by reference to the medians between 200 and 1300 CE, and between 300 and 800 CE, respectively (Fig. 4). Three cold intervals are recorded between 300 and 450 CE, 490 and 580 CE and between 700 and 780 CE. The indicated abrupt and maximum cooling at 330 CE is biased by the Ti-related flood peak. The largest differences between the two cores (represented by the standard deviation of Av. log(Ca/Ti), in grey in Fig. 4) during this coldest period support the hypothesis that the Ca record is temperature related. Cold temperatures can limit carbonate accumulation (Gierlowski-Kordesch, 2010). During cold periods, the production of algae declines, which in turn might increase the variability in the sediments of the lake leading to the difference in the Ca/Ti ratio between the two sediment cores. It is also likely that the building of the Raknehaugen burial mound on the shore of the lake locally affected the sedimentation and thus the climate signal derived from the core. For example, the transport of trunks to build the mound might have spread branches over the frozen lake, or more floating debris, resulting in the random deposit of additional terrestrial plant remains in the sediment, locally disturbing the sedimentation. Comparison of the Ca/Ti record with the data from Ljungqvist (2010) and Christiansen and Ljungqvist (2012) shows that the ^{14}C age model of Lake Ljøgottjern sediment sequence is accurate despite the uncertainties when using only radiocarbon dates in the model (Fig. 2).

4.4. Socio-environmental interactions between 200 and 1300 CE

The third century is characterised by warm temperatures, which allowed the cultivation of *Hordeum/Avena* in the vicinity of Lake Ljøgottjern (Fig. 3). The concentration of charcoals indicates regular fire activity, which could be related to land clearing and slash-and-burn agriculture. The *Sordaria* concentration in the sediment can be linked to the development of grazing activities. Ascospores of *Sordaria* develop on faeces of animals and are commonly use to trace the former local presence of herbivores and thus past husbandry as recorded in lake sediments and archaeological settlements (van Geel et al., 2003; Doyen and Etienne, 2017; Bajard et al., 2017). *Sordaria* is commonly associated with pollen of *Rumex*, Urticaceae and Poaceae, which are also grazing indicators (Doyen and Etienne, 2017).

Both the geochemistry and the palynological data show a profound change at c. 800 CE. This change reflects a major socio-environmental transition, which can be linked to the increase in temperature, and marks the transition from the Dark Ages Cold Period into the Viking Age (800–1000 CE).

During the Dark Ages the sediment of Ljøgottjern indicate cultivation of hemp (*Cannabis*). Hemp was primarily used for coarse textiles and ropes (Skoglund et al., 2013). The cultivation of hemp appeared around 400 CE and ended around 700 CE, before reappearing in the Viking Age.

In detail, the period 300–800 CE can be divided into intervals when farming practices were dominated by grazing, and intervals dominated by the cultivation of cereals and hemp. During 280–410, 480–580 and 700–780 CE the lake sediments were characterised by high concentrations of ascospores of *Sordaria,* and the percentages of pollen of *Rumex* and *Urtica* are also above the median. Pollen of *Plantago lanceolata* were found at 290, 320 and 420 CE, but might be very rare because of the climate (Sarmaja-Korjonen, 2003). Percentages of cultivated taxa remain below the median except for *Secale* in two samples, indicating a prevalence of husbandry activities over cultivation for these three intervals. By contrast, 410–480 and 580–700 CE present little evidence of grazing activities but percentages of pollen of *Cannabis*, *Secale, Triticum* or *Hordeum/Avena* are above the median, indicating a significant expansion of crop cultivation.

Spruce (*Picea*) increased until 550 CE. *Picea* is typically associated with an increase in human activities, which create openings for spruce to settle (Bjune et al., 2009). Percentage of *Picea* pollen increase because spruce replaces the other trees. Nettle (*Urtica*) develops in areas enriched in nitrogen, induced by the dejection of animals. The enrichment of the soil in nitrogen is therefore more important, where animals were staying for a long time, such as around buildings, around the lake, where animals might have come to drink, and along footpaths. The continuous occurrence of nettle between 400 and 550 CE suggests there were large numbers of people and animals inhabiting the area around the lake. Aquatic plants are sensitive to human presence and related nutrient inputs. Between 350 and 500 CE, high inputs of nutrients may have favoured the development of *Potamogeton* leading to the decrease in *Nymphaea*. The flood at c. 330 CE could have triggered a large nutrient input, increasing the lake level and thus favouring *Potamogeton* (Fig. 2).

The period from 680 to 800 CE presents less evidence for both grazing and cultivated taxa than the previous phases (Fig. 3). This is in agreement with the widespread abandonment evidenced in archaeological and lake records during the period 550–800 CE (Solberg, 1998; D'Anjou et al., 2012; Iversen, 2016). A possible abandonment at the present site is supported by the development of shrubs, as *Juniperus* (Supplementary Fig. 2), and the pioneer *Betula* and *Alnus*, which are known to colonise abandoned fields (Fig. 3). The period is also characterised by a slight recovery of *Nymphaea* that supports the hypothesis of a decrease in anthropic activities.

4.4.1. Alternation between animal husbandry and cultivation (300–800 CE)

Periods dominated by husbandry versus cultivation are shown in Fig. 4. The alternation of these periods between 300 and 800 CE coincides with the recorded changes in temperature (Fig. 4). Cold periods are associated with husbandry practices while warmer periods are associated with cultivation activities. To validate the assumption that the changes between husbandry and cultivation were related to changes in climate, we performed a Principal Component Analysis (PCA) on a selection of variables covering the period 200–850 CE. This included a selection of pollen, the concentrations in charcoal fragments and ascospores of *Sordaria*, the organic matter content and the reconstructed temperatures (Fig. 5). We did not extend the analysis into the period 850–1300 CE because the PCA was mainly reflecting the major transition at 850 CE.

The two first dimensions of the PCA (denoted Dim1 and Dim2 in Fig. 5) represent 38% of the variability in the dataset. Four endmembers are identified on the correlation circle (Fig. 5a). The first one is positively correlated to the first component of the PCA and yields high positive loadings for husbandry and land clearing (e.g. *Rumex longifolius, Rumex acetosa, Sordaria* fungi, *Alnus* and charcoals). The occurrence of husbandry and land clearing at the same time could be associated with instability of the human activity, alternating between abandonment and clearing of the space. *Alnus* is a pioneer species, which would be the first tree to recolonize the area if the human pressure decreased. *Alnus* is also an indicator of wet conditions and deterioration of the climate. A second endmember is negatively correlated with the first dimension and therefore to the first endmember. It allows the discrimination of the culture of *Triticum*, *Secale* and *Cannabis*. This first dimension can therefore be associated with changes in agricultural practices and demonstrates the opposition between husbandry practices and the cultivation of cereals and hemp. The second dimension of the PCA may be associated with climate change. A third endmember including the temperature proxy (log(Ca/Ti)), the organic matter, Poaceae and *Hordeum/Avena* is associated with the positive values of the second dimension. This pool is negatively correlated with *Pinus*, forming the fourth endmember, standing for abandonment, forested environment, and lower temperature. *Sordaria* fungi, *Rumex longifolius* and *Urtica* are closer to the negative values of the climate dimension while *Cannabis*, *Triticum* and *Secale* are closer to the temperature proxy (Fig. 5a). This disposition supports the hypothesis that changes in farming practices were driven by temperature changes. The culture of cereals and hemp needs relatively high temperatures and a defined growth period, which is not possible when the climate is colder, and thus, these colder periods are dominated by husbandry.

The individual factors map of the PCA shows the trajectories of evolution of the environment (Fig. 5b). It underlines the scenario of evolution where colder periods are associated with the abandonment of cultivation and adaptation of agricultural practices toward more livestock farming. The transitions from cold to warm periods show the resilience of society and onset of cultivation of cereals and hemp. The interval from 310 to 580 CE appears to be the coldest during the period between 200 and 850 CE. Finally, the change in agricultural practices can reflect an adaptation of society to the climate variability, rather than societal instability. The alternation and progressive decrease in anthropic evidence (concentration in *Sordaria*, percentage of pollen of cultivated taxa) through this period could also reflect the oscillation of the carrying capacity of

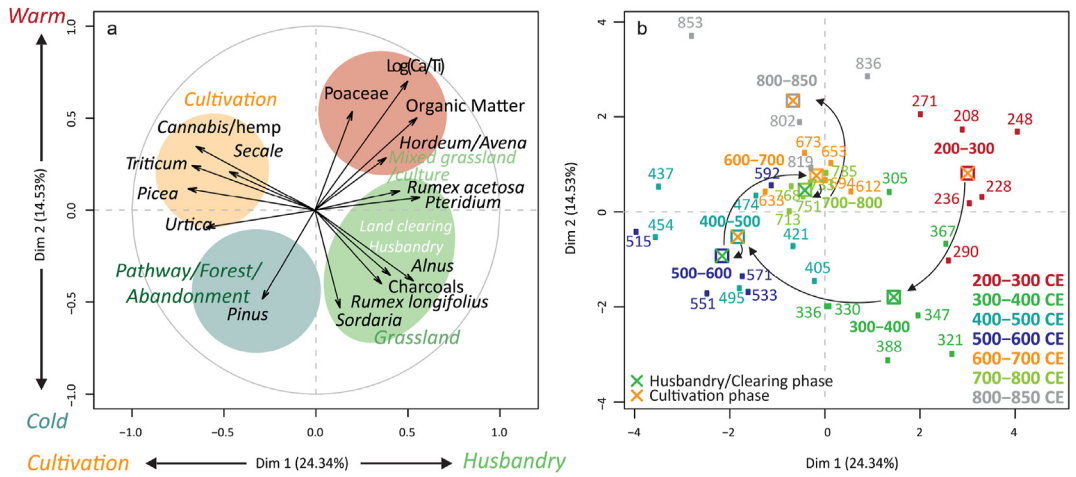

Fig. 5. Principal Component Analysis. a Correlation Circle **b** and map of the individuals of the PCA including selected taxa from the palynological analysis (Pinus, Picea, Cannabis, Secale, Triticum, Poaceae, Hordeum/Avena, Rumex acetosa, Rumex longifolius, Urtica, Pteridium, Alnus, the concentrations in charcoals and Sordaria fungi) plus the Log(Ca/Ti) and organic matter changes reconstructed from the XRF geochemistry.

the society and its degradation in the last centuries before the Viking Age. However, the suggested abandonment between 680 and 800 CE does not correspond to the coldest period and is therefore unlikely to be directly related to climate change. Other factors have to be taken into account, such as the Justinian Plague that impacted the population in Europe from 541 to 750 CE, the prevalence of an epidemic could be linked to climate variability (Little, 2007; Kausrud et al., 2010; Keller et al., 2019). More recently, the smallpox virus has been discovered in the remains of humans who were living in Norway and Sweden in the 7th century (Mühlemann et al., 2020) and could have contributed to the decrease of anthropic pressure during the end of the Dark Ages.

4.4.2. The Viking Age and onset of the Middle Ages

The Viking Age started with warmer climate in Scandinavia in c. 800 CE (Fig. 4), which allowed rapid development of agricultural practices. This major change is visible in a large range of taxa (Fig. 3). *Pinus* reached a minimum around 900 CE and *Betula* and *Alnus* also decreased, while *Picea* and *Urtica* increased again, suggesting an even larger opening up of the landscape than previously. Large amounts of *Cannabis* pollen are recorded after 900 CE, indicating that the lake was being used for hemp retting. In the Viking Age and early Middle Ages, hemp was produced in several places in Norway and Sweden (Skoglund et al., 2013; Wieckowska-Lüth et al., 2017). The production of flax is also recorded during the Viking Age. *Secale*, *Triticum* and *Hordeum/Avena* were all cultivated during the warmest period 950–1000 CE and regularly recorded above median between 850 and 1300 CE. The disappearance of *Nymphaea,* replaced by *Potamogeton* points to an increase in nutrient inputs to the lake, as a result of a new increase in human activities. The start of the Middle Ages (c. 1000 CE) is characterised by a slight decrease in temperature associated with more grazing activities than in the Viking Age. The fire regime activity is also more prominent. Through the period 200–1300 CE, fires appear to coincide with grazing activities, suggesting the use of fire to clear the land and maintain areas opened. A comparison with other charcoal records in the same area (within 20 km radius) suggests that Lake Ljøgottjern recorded local fire activity (Høeg, 1997). Nevertheless, the period from The Viking Age to the High Middle Ages (c. 800–1300 CE) was a period of expansion with the Viking diaspora, increasing trade, food and goods production and the establishment of Scandinavian towns (e.g. Kuitems et al., 2021). This period also sees a rapid increase in population and settlements, mainly due to a relatively stable warm climate (McEvedy et al., 1978; Benedictow, 1996; Barrett, 2008).

5. Conclusion

Overall, these findings suggest that temperature was the main driver of agricultural practices in Southeastern Norway during the Late Antiquity. Direct comparison between the reconstructed temperature variability and palynological data from the same sediment sequence shows that small changes in temperature were synchronous with changes in agricultural practices (husbandry during cold periods, cultivation during warm periods) during the Dark Ages Cold Period. We conclude that the pre-Viking age society in Southwestern Scandinavia made substantial changes in their way of living to adapt to the climate variability of this period. To further constrain the observations in this paper and to study the spatial variability it is needed with more reconstructions based on our approach. Combining proxy reconstructions with paleo model experiments based on earth system models would significantly increase our understating of the linkages between human activity and climate through time.

Author contributions

M.B., K.K., H.S., J.B., F.I. and A.J. designed research; M.B, E.B., H.H, J.B., E.S., K.L. and W.H. performed research; M.B, H.H, W.H. and K.L. analysed data; and M.B., K.K., J.B., H.S., F.I., K.L., W.H. wrote the paper.

Data availability

The data related to this study will be published at www.pangaea.de after acceptance of the manuscript.

Declaration of competing interest

The authors declare that they have no known competing financial interests or personal relationships that could have appeared to influence the work reported in this paper.

Acknowledgments

This work is part of the VIKINGS project “Volcanic Eruptions and

their Impacts on Climate, Environment, and Viking Society in 500–1250 CE", funded as a FRIPRO Toppforsk project by the Research Council of Norway (project number 275191). The two coring campaigns, the XRF geochemistry and LOI were conducted within the National Infrastructure EARTHLAB (NRC 226171) at the University of Bergen and the CLIPT lab at the University of Oslo. This work was supported by the Research Council of Norway Centres of Excellence CEED project 223272. We thank Michael Sigl for the fruitful discussion and advice on the climate proxy data.

Appendix A. Supplementary data

Supplementary data to this article can be found online at https://doi.org/10.1016/j.quascirev.2022.107374.

References

Adrian, R., O'Reilly, C.M., Zagarese, H., Baines, S.B., Hessen, D.O., Keller, W., Livingstone, D.M., Sommaruga, R., Straile, D., Van Donk, E., Weyhenmeyer, G.A., Winder, M., 2009. Lakes as sentinels of climate change. Limnol. Oceanogr. 54, 2283–2297. https://doi.org/10.4319/lo.2009.54.6_part_2.2283.

Arnaud, F., Poulenard, J., Giguet-Covex, C., Wilhelm, B., Révillon, S., Jenny, J.-P., Revel, M., Enters, D., Bajard, M., Fouinat, L., others, 2016. Erosion under climate and human pressures: an alpine lake sediment perspective. Quat. Sci. Rev. 152, 1–18.

Bajard, M., Poulenard, J., Sabatier, P., Etienne, D., Ficetola, F., Chen, W., Gielly, L., Taberlet, P., Develle, A.-L., Rey, P.-J., Moulin, B., Beaulieu, J., Arnaud, F., 2017. Long-term changes in alpine pedogenetic processes: effect of millennial agro-pastoralism activities (French-Italian Alps). Geoderma 306, 217–236. https://doi.org/10.1016/j.geoderma.2017.07.005.

Bajard, M., Sabatier, P., David, F., Develle, A.-L., Reyss, J.-L., Fanget, B., Malet, E., Arnaud, D., Augustin, L., Crouzet, C., Poulenard, J., Arnaud, F., 2016. Erosion record in lake La thuile sediments (prealps, France): evidence of montane landscape dynamics throughout the Holocene. Holocene 26, 350–364.

Barrett, J.H., 2008. What caused the viking age? Antiquity 82, 671–685. https://doi.org/10.1017/S0003598X00097301.

Benedictow, O.J., 1996. The demography of the viking age and the high Middle ages in the nordic countries. Scand. J. Hist. 21, 151–182.

Beug, H.-J., 1961. Leitfaden der Pollenbestimmung für Mitteleuropa und angrenzende Gebiete: Mit 17 Abbildungen und 8 Tafeln. G. Fischer.

Bjune, A.E., Ohlson, M., Birks, H.J.B., Bradshaw, R.H.W., 2009. The development and local stand-scale dynamics of a Picea abies forest in southeastern Norway. Holocene 19, 1073–1082. https://doi.org/10.1177/0959683609341004.

Blaauw, M., Christen, J.A., 2011. Flexible paleoclimate age-depth models using an autoregressive gamma process. Bayesian Anal 6, 457–474. https://doi.org/10.1214/11-BA618.

Bøe, A.-G., Dahl, S.O., Lie, Ø., Nesje, A., 2006. Holocene river floods in the upper Glomma catchment, southern Norway: a high-resolution multiproxy record from lacustrine sediments. Holocene 16, 445–455. https://doi.org/10.1191/0959683606hl940rp.

Bonk, A., Müller, D., Ramisch, A., Kramkowski, M.A., Noryśkiewicz, A.M., Sekudewicz, I., Gąsiorowski, M., Luberda-Durnaś, K., Słowiński, M., Schwab, M., Tjallingii, R., Brauer, A., Błaszkiewicz, M., 2021. Varve microfacies and chronology from a new sediment record of Lake Gościąż (Poland). Quat. Sci. Rev. 251, 106715. https://doi.org/10.1016/j.quascirev.2020.106715.

Büntgen, U., Myglan, V.S., Ljungqvist, F.C., McCormick, M., Di Cosmo, N., Sigl, M., Jungclaus, J., Wagner, S., Krusic, P.J., Esper, J., Kaplan, J.O., de Vaan, M.A.C., Luterbacher, J., Wacker, L., Tegel, W., Kirdyanov, A.V., 2016. Cooling and societal change during the late Antique little ice age from 536 to around 660 AD. Nat. Geosci. 9, 231–236. https://doi.org/10.1038/ngeo2652.

Buntgen, U., Tegel, W., Nicolussi, K., McCormick, M., Frank, D., Trouet, V., Kaplan, J.O., Herzig, F., Heussner, K.U., Wanner, H., Luterbacher, J., Esper, J., 2011. 2500 Years of European climate variability and human susceptibility. Science 331, 578–582. https://doi.org/10.1126/science.1197175.

Büntgen, U., Urban, O., Krusic, P.J., Rybníček, M., Kolář, T., Kyncl, T., Ač, A., Koňasová, E., Čáslavský, J., Esper, J., Wagner, S., Saurer, M., Tegel, W., Dobrovolný, P., Cherubini, P., Reinig, F., Trnka, M., 2021. Recent European drought extremes beyond Common Era background variability. Nat. Geosci. https://doi.org/10.1038/s41561-021-00698-0.

Christiansen, B., Ljungqvist, F.C., 2012. The extra-tropical Northern Hemisphere temperature in the last two millennia: reconstructions of low-frequency variability. Clim. Past 8, 765–786. https://doi.org/10.5194/cp-8-765-2012.

Costanza, R., Graumlich, L., Steffen, W., Crumley, C., Dearing, J., Hibbard, K., Leemans, R., Redman, C., Schimel, D., 2007. Sustainability or collapse: what can we learn from integrating the history of humans and the rest of nature? AMBIO A J. Hum. Environ. 36, 522–527.

Cugny, C., Mazier, F., Galop, D., 2010. Modern and fossil non-pollen palynomorphs from the Basque mountains (western Pyrenees, France): the use of coprophilous fungi to reconstruct pastoral activity. Veg. Hist. Archaeobotany 19, 391–408. https://doi.org/10.1007/s00334-010-0242-6.

D'Anjou, R.M., Bradley, R.S., Balascio, N.L., Finkelstein, D.B., 2012. Climate impacts on human settlement and agricultural activities in northern Norway revealed through sediment biogeochemistry. Proc. Natl. Acad. Sci. Unit. States Am. 109, 20332–20337. https://doi.org/10.1073/pnas.1212730109.

Davaud, E., Girardclos, S., 2001. Recent freshwater ooids and oncoids from western Lake Geneva (Switzerland): indications of a common organically mediated origin. J. Sediment. Res. 71, 423–429.

Dean Jr., W.E., 1974. Determination of carbonate and organic matter in calcareous sediments and sedimentary rocks by loss on ignition: comparison with other methods. SEPM J. Sediment. Res. 44. https://doi.org/10.1306/74D729D2-2B21-11D7-8648000102C1865D.

Directorate for Cultural Heritage, 2020. Norwegian national heritage database. Available online: https://askeladden.ra.no/Askeladden/Pages/LoginPage.aspx?ReturnUrl=%2faskeladden (accessed in 2020).

Doyen, E., Etienne, D., 2017. Ecological and human land-use indicator value of fungal spore morphotypes and assemblages. Veg. Hist. Archaeobotany 26, 357–367. https://doi.org/10.1007/s00334-016-0599-2.

Engeland, K., Aano, A., Steffensen, I., Støren, E., Paasche, Ø., 2020. New flood frequency estimates for the largest river in Norway based on the combination of short and long time series (preprint). Catchment hydrology/Instruments and observation techniques. https://doi.org/10.5194/hess-2020-269.

Engeland, K., Wilson, D., Borsányi, P., Roald, L., Holmqvist, E., 2018. Use of historical data in flood frequency analysis: a case study for four catchments in Norway. Nord. Hydrol 49, 466–486. https://doi.org/10.2166/nh.2017.069.

Etienne, D., Wilhelm, B., Sabatier, P., Reyss, J.-L., Arnaud, F., 2013. Influence of sample location and livestock numbers on Sporormiella concentrations and accumulation rates in surface sediments of Lake Allos, French Alps. J. Paleolimnol. 49, 117–127. https://doi.org/10.1007/s10933-012-9646-x.

Faegri, K., Iversen, J., 1989. Textbook of Pollen Analysis, Revised by Faegri K, Kaland PE. J Wiley N. Y, Krzywinski K.

Faegri, K., Iversen, J., 1966. Textbook of Pollen Analysis. Kobenhavn.

Galka, B., Labaz, B., Bogacz, A., Bojko, O., Kabala, C., 2014. Conversion of Norway spruce forests will reduce organic carbon pools in the mountain soils of SW Poland. Geoderma 213, 287–295. https://doi.org/10.1016/j.geoderma.2013.08.029.

Gierlowski-Kordesch, E.H., 2010. Chapter 1 lacustrine carbonates. In: Developments in Sedimentology. Elsevier, pp. 1–101. https://doi.org/10.1016/S0070-4571(09)06101-9.

Grieg, S., 1940. Innberetning Angående Raknehaugundersøkelsen 1. juni Topark.

Haug, G.H., Gunther, D., Peterson, L.C., Sigman, D.M., Hughen, K.A., Aeschlimann, B., 2003. Climate and the Collapse of Maya Civilization 299, 6.

Helama, S., Jones, P.D., Briffa, K.R., 2017a. Dark Ages Cold Period: a literature review and directions for future research. Holocene 27, 1600–1606. https://doi.org/10.1177/0959683617693898.

Helama, S., Jones, P.D., Briffa, K.R., 2017b. Limited late Antique cooling. Nat. Geosci. 10, 242–243. https://doi.org/10.1038/ngeo2926.

Helliksen, W., 1997. Gård og utmark på romerrike 1100 f. Kr.-1400 e. Kr: Gardermoprosjektet. Universitetets Oldsaksamling.

Høeg, H.I., 1997. Pollenanalytiske Undersøkelser På Øvre Romerike : Ullensaker Og Nannestad, Akershus Fylke : Gardermoprosjektet, Varia (Universitetets Oldsaksamling : Trykt Utg. Universitetets oldsaksamling, Oslo.

Iversen, F., 2016. Estate division: social cohesion in the aftermath of 536-7 35.

Johnsen, J., 1943. Årringsanalyser på trevirke fra Raknehaugen. Hovedoppgave i botanikk, Upublisert.

Kausrud, K.L., Begon, M., Ari, T.B., Viljugrein, H., Esper, J., Büntgen, U., Leirs, H., Junge, C., Yang, B., Yang, M., others, 2010. Modeling the epidemiological history of plague in Central Asia: palaeoclimatic forcing on a disease system over the past millennium. BMC Biol. 8, 112.

Keller, M., Spyrou, M.A., Scheib, C.L., Neumann, G.U., Kröpelin, A., Haas-Gebhard, B., Päffgen, B., Haberstroh, J., Ribera i Lacomba, A., Raynaud, C., Cessford, C., Durand, R., Stadler, P., Nägele, K., Bates, J.S., Trautmann, B., Inskip, S.A., Peters, J., Robb, J.E., Kivisild, T., Castex, D., McCormick, M., Bos, K.I., Harbeck, M., Herbig, A., Krause, J., 2019. Ancient Yersinia pestis genomes from across western Europe reveal early diversification during the first pandemic (541–750). Proc. Natl. Acad. Sci. Unit. States Am. 116, 12363–12372. https://doi.org/10.1073/pnas.1820447116.

Königsson, L.-K., 1968. The Holocene History of the Great Alvar of Öland (PhD Thesis). Sv. växtgeografiska sällsk.

Kotov, S., Paelike, H., 2018. QAnalySeries-a cross-platform time series tuning and analysis tool. AGUFM, 2018, PP53D-1230.

Kuitems, M., Wallace, B.L., Lindsay, C., Scifo, A., Doeve, P., Jenkins, K., Lindauer, S., Erdil, P., Ledger, P.M., Forbes, V., Vermeeren, C., Friedrich, R., Dee, M.W., 2021. Evidence for European presence in the Americas in ad 1021. Nature. https://doi.org/10.1038/s41586-021-03972-8.

Kupryjanowicz, M., 2007. Postglacial development of vegetation in the vicinity of the wigry lake. GEOCHR 27, 53–66. https://doi.org/10.2478/v10003-007-0018-x.

Lid, J., Lid, D., 1994. Norsk Flora. 6. Utgave. Det Nor. Saml, Oslo.

Little, L.K., 2007. Plague and the End of Antiquity: the Pandemic of 541-750. Cambridge University Press.

Ljungqvist, F.C., 2010. A new reconstruction of temperature variability in the extra-tropical northern hemisphere during the last two millennia. Geogr. Ann. Ser. Phys. Geogr. 92, 339–351. https://doi.org/10.1111/j.1468-0459.2010.00399.x.

Longva, O., Thoresen, M.K., 1989. The age of the Hauerseter delta. Nor. Geol. Tidsskr. 69, 131–134.

Lücke, A., Schleser, G.H., Zolitschka, B., Negendank, J.F., 2003. A Lateglacial and Holocene organic carbon isotope record of lacustrine palaeoproductivity and climatic change derived from varved lake sediments of Lake Holzmaar, Germany. Quat. Sci. Rev. 22, 569–580.

Luterbacher, J., Werner, J.P., Smerdon, J.E., Fernández-Donado, L., González-Rouco, F.J., Barriopedro, D., Ljungqvist, F.C., Büntgen, U., Zorita, E., Wagner, S., Esper, J., McCarroll, D., Toreti, A., Frank, D., Jungclaus, J.H., Barriendos, M., Bertolin, C., Bothe, O., Brázdil, R., Camuffo, D., Dobrovolný, P., Gagen, M., García-Bustamante, E., Ge, Q., Gómez-Navarro, J.J., Guiot, J., Hao, Z., Hegerl, G.C., Holmgren, K., Klimenko, V.V., Martín-Chivelet, J., Pfister, C., Roberts, N., Schindler, A., Schurer, A., Solomina, O., von Gunten, L., Wahl, E., Wanner, H., Wetter, O., Xoplaki, E., Yuan, N., Zanchettin, D., Zhang, H., Zerefos, C., 2016. European summer temperatures since Roman times. Environ. Res. Lett. 11, 024001. https://doi.org/10.1088/1748-9326/11/2/024001.

McEvedy, C., Jones, R., others, 1978. Atlas of World Population History. Penguin Books Ltd, Harmondsworth, Middlesex, England.

Meyers, P.A., Teranes, J.L., 2002. Sediment organic matter. In: Last, W.M., Smol, J.P. (Eds.), Tracking Environmental Change Using Lake Sediments, Developments in Paleoenvironmental Research. Kluwer Academic Publishers, Dordrecht, pp. 239–269. https://doi.org/10.1007/0-306-47670-3_9.

Mommsen, T.E., 1942. Petrarch's conception of the "dark ages. Speculum 17, 226–242. https://doi.org/10.2307/2856364.

Mühlemann, B., Vinner, L., Margaryan, A., Wilhelmson, H., 2020. Diverse variola Virus (Smallpox) Strains Were Widespread in Northern Europe in the Viking Age 12.

Nesje, A., 1992. A piston corer for lacustrine and marine sediments. Arct. Alp. Res. 24, 257. https://doi.org/10.2307/1551667.

Nesje, A., Dahl, S.O., Matthews, J.A., Berrisford, M.S., 2001. Ã 4500 yr record of river floods obtained from a sediment core in Lake Atnsjøen, eastern Norway. J. Paleolimnol. 25, 329–342.

Newfield, T.P., 2018. The climate downturn of 536–50. In: White, S., Pfister, C., Mauelshagen, F. (Eds.), The Palgrave Handbook of Climate History. Palgrave Macmillan UK, London, pp. 447–493. https://doi.org/10.1057/978-1-137-43020-5_32.

Niinemets, E., Saarse, L., Poska, A., 2002. Vegetation history and human impact in the Parika area, Central Estonia. In: Proceedings of the Estonian Academy of Sciences, pp. 241–258. Geology.

Nydal, R., 1959. Trondheim natural radiocarbon measurements I. Radiocarbon 1, 76–80. https://doi.org/10.1017/S0033822200020385.

O'Beirne, M.D., Werne, J.P., Hecky, R.E., Johnson, T.C., Katsev, S., Reavie, E.D., 2017. Anthropogenic climate change has altered primary productivity in Lake Superior. Nat. Commun. 8, 15713. https://doi.org/10.1038/ncomms15713.

Ording, A., 1941. Skoghistoriske analyser fra Raknehaugen. For. Hist. Anal. Raknehaugen Medd Nor. Slc0gsf0rs¢ Ksvesen 3, 27.

Orlove, B., 2005. Human adaptation to climate change: a review of three historical cases and some general perspectives. Environ. Sci. Pol. 8, 589–600. https://doi.org/10.1016/j.envsci.2005.06.009.

Peregrine, P.N., 2020. Climate and social change at the start of the late Antique little ice age. Holocene. https://doi.org/10.1177/0959683620941079, 095968362094107.

Reimer, P.J., Austin, W.E.N., Bard, E., Bayliss, A., Blackwell, P.G., Bronk Ramsey, C., Butzin, M., Cheng, H., Edwards, R.L., Friedrich, M., Grootes, P.M., Guilderson, T.P., Hajdas, I., Heaton, T.J., Hogg, A.G., Hughen, K.A., Kromer, B., Manning, S.W., Muscheler, R., Palmer, J.G., Pearson, C., van der Plicht, J., Reimer, R.W., Richards, D.A., Scott, E.M., Southon, J.R., Turney, C.S.M., Wacker, L., Adolphi, F., Büntgen, U., Capano, M., Fahrni, S.M., Fogtmann-Schulz, A., Friedrich, R., Köhler, P., Kudsk, S., Miyake, F., Olsen, J., Reinig, F., Sakamoto, M., Sookdeo, A., Talamo, S., 2020. The INTCAL20 Northern Hemisphere radiocarbon age calibration curve (0–55 CAL kBP). Radiocarbon 1–33. https://doi.org/10.1017/RDC.2020.41.

Riechelmann, D.F.C., Gouw-Bouman, M.T.I.J., 2018. A review of climate reconstructions from terrestrial climate archives covering the first millennium AD in northwestern Europe. Quat. Res. 1–21. https://doi.org/10.1017/qua.2018.84.

Sarmaja-Korjonen, K., 2003. Contemporaneous Alnus decline and the beginning of Iron Age cultivation in pollen stratigraphies from southern Finland. Veg. Hist. Archaeobotany 12, 49–59. https://doi.org/10.1007/s00334-003-0005-8.

Shumilovskikh, L.S., van Geel, B., 2020. Non-pollen palynomorphs. In: Handbook for the Analysis of Micro-particles in Archaeological Samples. Springer, pp. 65–94.

Sigl, M., McConnell, J.R., Toohey, M., Curran, M., Das, S.B., Edwards, R., Isaksson, E., Kawamura, K., Kipfstuhl, S., Krüger, K., Layman, L., Maselli, O.J., Motizuki, Y., Motoyama, H., Pasteris, D.R., Severi, M., 2014. Insights from Antarctica on volcanic forcing during the Common Era. Nat. Clim. Change 4, 693–697. https://doi.org/10.1038/nclimate2293.

Sigl, M., Winstrup, M., McConnell, J.R., Welten, K.C., Plunkett, G., Ludlow, F., Büntgen, U., Caffee, M., Chellman, N., Dahl-Jensen, D., Fischer, H., Kipfstuhl, S., Kostick, C., Maselli, O.J., Mekhaldi, F., Mulvaney, R., Muscheler, R., Pasteris, D.R., Pilcher, J.R., Salzer, M., Schüpbach, S., Steffensen, J.P., Vinther, B.M., Woodruff, T.E., 2015. Timing and climate forcing of volcanic eruptions for the past 2,500 years. Nature. https://doi.org/10.1038/nature14565.

Skoglund, G., Nockert, M., Holst, B., 2013. Viking and early Middle ages northern scandinavian textiles proven to be made with hemp. Sci. Rep. 3. https://doi.org/10.1038/srep02686.

Skre, D., 1997. Raknehaugen. En Empirisk Loftsrydding, vol. 38.

Solberg, B., 1998. Settlement and social structure in Norway in the Migration period (AD 400–550). Archaeol. Balt. 3, 235–250.

Stabel, H.-H., 1986. Calcite precipitation in Lake Constance: chemical equilibrium, sedimentation, and nucleation by algae1: calcite sedimentation. Limnol. Oceanogr. 31, 1081–1094. https://doi.org/10.4319/lo.1986.31.5.1081.

Stancikaite, M., Kisielienė, D., Strimaitienė, A., 2004. Vegetation response to the climatic and human impact changes during the Late Glacial and Holocene: case study of the marginal area of Baltija Upland, NE Lithuania. Baltica 17, 17–33.

Stockmarr, J., 1971. Tablets with Spores Used in Absolute Pollen Analysis (Pollen Spores).

Støren, E.N., Paasche, Ø., 2014. Scandinavian floods: from past observations to future trends. Global Planet. Change 113, 34–43. https://doi.org/10.1016/j.gloplacha.2013.12.002.

Sugita, S., 1994. Pollen representation of vegetation in quaternary sediments: theory and method in patchy vegetation. J. Ecol. 82, 881. https://doi.org/10.2307/2261452.

ter Schure, A.T.M., Bajard, M., Loftsgarden, K., Høeg, H.I., Ballo, E., Bakke, J., Støren, E.W.N., Iversen, F., Kool, A., Brysting, A.K., Krüger, K., Boessenkool, S., 2021. Anthropogenic and environmental drivers of vegetation change in southeastern Norway during the Holocene. Quat. Sci. Rev. 270, 107175. https://doi.org/10.1016/j.quascirev.2021.107175.

Theroux, S., D'Andrea, W.J., Toney, J., Amaral-Zettler, L., Huang, Y., 2010. Phylogenetic diversity and evolutionary relatedness of alkenone-producing haptophyte algae in lakes: implications for continental paleotemperature reconstructions. Earth Planet Sci. Lett. 300, 311–320. https://doi.org/10.1016/j.epsl.2010.10.009.

Toohey, M., Krüger, K., Sigl, M., Stordal, F., Svensen, H., 2016. Climatic and societal impacts of a volcanic double event at the dawn of the Middle Ages. Clim. Change 136, 401–412. https://doi.org/10.1007/s10584-016-1648-7.

Tvauri, A., 2014. The impact of the climate catastrophe of 536-537 AD in Estonia and neighbouring areas. Est. J. Archaeol. 18, 30. https://doi.org/10.3176/arch.2014.1.02.

van Geel, B., Buurman, J., Brinkkemper, O., Schelvis, J., Aptroot, A., van Reenen, G., Hakbijl, T., 2003. Environmental reconstruction of a Roman Period settlement site in Uitgeest (The Netherlands), with special reference to coprophilous fungi. J. Archaeol. Sci. 11.

Weltje, G.J., Tjallingii, R., 2008. Calibration of XRF core scanners for quantitative geochemical logging of sediment cores: theory and application. Earth Planet Sci. Lett. 274, 423–438. https://doi.org/10.1016/j.epsl.2008.07.054.

Wickler, S., Narmo, L.E., 2014. Tracing the development of fishing settlement from the iron age to the modern Period in northern Norway: a case study from borgvær in the lofoten islands. J. Isl. Coast. Archaeol. 9, 72–87.

Widgren, M., 2012. Climate and causation in the Swedish Iron Age: learning from the present to understand the past. Geogr. Tidsskr.-Dan. J. Geogr. 112, 126–134. https://doi.org/10.1080/00167223.2012.741886.

Wieckowska-Lüth, M., Kirleis, W., Doerfler, W., 2017. Holocene history of landscape development in the catchment of Lake Skogstjern, southeastern Norway, based on a high-resolution multi-proxy record. Holocene 27, 1928–1947. https://doi.org/10.1177/0959683617715691.